Xi'an Shiyou Daxue Xuebao (Ziran Kexue Ban)/
Journal of Xi'an Shiyou University, Natural Sciences Edition
ISSN: 1673-064X
E-Publication: Online Open Access
Vol: 68 Issue 01 | 2025
DOI: 10.5281/zenodo.14752620

IRIS CONTOUR DETECTION USING OTSU HYSTERISIS THRESHOLDING

KAMEL GHANEM GHALEM
Complex System Laboratory, Higher School of Electrical and Energetic Engineering, Oran, Algeria.

ALI BENOUAR*
Complex System Laboratory, Higher School of Electrical and Energetic Engineering, Oran, Algeria.
*Corresponding Author

KAMILA ALIANE
Complex System Laboratory, Higher School of Electrical and Energetic Engineering, Oran, Algeria.

YASMINA ZINE
University of Science and Technology of Oran Mohamed Boudiaf, USTO-MB.

MOHAMED REDA AHMED BACHA
Complex System Laboratory, Higher School of Electrical and Energetic Engineering, Oran, Algeria.

Abstract

This work introduces a new method to improve iris contour identification, especially for iris images taken in a constrained environment, by combining the Otsu method with hysteresis local thresholding. The iris segmentation is processed on the whole iris disc. A competitive method called the Dezert-Smarandache hypothesis is used to apply the fusion of the left and right iris at the score level. Using the challenging CASIA-IrisV4 Interval database, the proposed approach demonstrated encouraging results with an accuracy of 94.06%, a False Acceptance Rate (FAR) of 5.83%, a False Rejection Rate (FRR) of 20.41%, and an Equal Error Rate (EER) of 20.7%.

Keywords: Biometric, Iris, Thresholding Method, Dezert Smarandache Theory.

1. INTRODUCTION

Because of its low error rates, the iris is considered as one of the most reliable and efficient biometric modalities. The main circumstances in which this great degree of precision has been attained are controlled ones, where acquisition limitations guarantee excellent image capture.

However, even a partial relaxation of these restrictions frequently results in a deterioration of image quality, which lowers the overall effectiveness of biometric systems. Improving the iris segmentation process is one of the main strategies in the literature to overcome these issues [1].

A key method in image processing for image segmentation is thresholding, which turns grayscale images into binary images. In order to distinguish between foreground and background areas, a threshold value must be defined. New global and local thresholding techniques have been developed recently to improve segmentation accuracy.

Xi'an Shiyou Daxue Xuebao (Ziran Kexue Ban)/
Journal of Xi'an Shiyou University, Natural Sciences Edition
ISSN: 1673-064X
E-Publication: Online Open Access
Vol: 68 Issue 01 | 2025
DOI: 10.5281/zenodo.14752620

1.1 Global Thresholding Method

To obtain the optimal threshold, the Otsu [2] technique minimizes the weighted sum of intra-class variances for both the background and foreground. Reducing intra-class variance is equivalent to increasing inter-class variance, or the distance between classes. When the number of pixels in each class is about equal, this method yields satisfactory results. The Otsu method is one of the most often used thresholding strategies. Velasco [3] uses isodata clustering to examine thresholding. However, Lee and Liu's investigation revealed flaws in the Otsu approach. To address some of these concerns, Li [4] extended the concept to a two-dimensional Otsu algorithm. Global thresholding applies a single threshold value to the entire image. Elen's Thresholding [5] is an innovation.

It is a histogram-based technique that uses the mean and standard deviation of an image's histogram to establish the ideal threshold values. Images with different distributions of intensity can be successfully segmented thanks tothis method.

Another significant advance is the Tsallis entropy-based thresholding approach [6]. This method improves performance in images with complex intensity distributions by setting threshold values based on the information theory concept of entropy. Yen's approach [7] optimizes the sum of squared probabilities for the divided classes. Its primary purpose is to keep the histogram peaks intact throughout segmentation.

Li's Cross Entropy Minimum [8]: The cross-entropy between the binary segmented image and the original grayscale image is reduced by thresholding. To ensure that there is no information loss during thresholding, the Cross-entropy evaluates the divergence between two probability distributions.

Kapur's technique [9] uses Shannon's entropy to maximize information content between foreground and background. The optimal threshold is determined by calculating the value that maximizes the sum of the entropies of the two classes.

In order to help COVID-19 detection, this study [10] segments lung regions and looks for white spots in chest X-ray images using the Otsu and and Phansalkar thresholding approaches.

1.2 Local Thresholding Methods

Local thresholding works effectively with images with uneven lighting or various textures since the method provides different threshold values to each pixel based on its local neighborhood. Current techniques include:

- Nick's Binarization that was improved by Niblack's approach [11] thanks to a downward threshold binary shifting and modifying the thresholding formula so as to optimize the image binarization with light backgrounds.
- Adaptive Thresholding using Local Binary Patterns (LBP) [12], a technique that enhances segmentation accuracy, particularly in remote sensing picture reconstruction, by combining adaptive thresholding with LBP features.

Xi'an Shiyou Daxue Xuebao (Ziran Kexue Ban)/
Journal of Xi'an Shiyou University, Natural Sciences Edition
ISSN: 1673-064X
E-Publication: Online Open Access
Vol: 68 Issue 01 | 2025
DOI: 10.5281/zenodo.14752620

- Similar to Niblack's approach, Sauvola'sthresholding method [13] dynamically determines the threshold using local statistics, but it additionally includes a term and takes into account the dynamic range of image intensities.
- By averaging the maximum and least intensity values in a neighborhood, Bernsen's method [14] determines the threshold and calculates the contrast within that neighborhood. If the contrast drops below a preset threshold, the global average intensity is applied to the pixel.
- Roth, Bradley using adaptive thresholding[15], the threshold is determined by subtracting a constant from the average pixel intensity in a local region.
- Multi-Scale Local Thresholding Based on Class Uncertainty Theory [16]: This method uses a multi-layer pyramid structure to split the original image into sub-regions of various scales, enabling more accurate segmentation by taking class uncertainty into account at several scales.

This study [17] segments X-ray thorax images using the Bradley thresholding approach to extract morphological information relevant to COVID-19 detection.

This paper proposes a novel thresholding method combining the Otsu and hysteresis-based local thresholding, two well-known methodologies. We also investigate other thresholding techniques, such as the Otsu and adaptive thresholding, which resist low contrast, specular reflections, and lighting variations found in iris images in an uncontrolled environment. We provide a detailed analysis and comparative assessment of different approaches. This paper is organized into the subsequent sections: Section II describes thresholding literature, Section III explains a proposed approach. Section IV presents the results and discussion.

2. THE COMPREHENSIVE THEORETICAL BASIS

In the literature, techniques that use gradient analysis to find local maxima compute an image's gradient magnitude to create an edge map. Following the creation of the edge map, contour information is clarified by applying thresholding. White pixels (value: 1) indicate contours in the final binary (black and white) picture, whereas black pixels (value: 0) indicate non-contour regions. The threshold parameter, S, must be set as follows for this thresholding process:

$$I_b(i,j) = \begin{cases} 1 \; si \; I_M(i,j) \geq S \\ 0 \quad sinon \end{cases} \qquad (1)$$

In the first technique, the threshold is determined by trial and error, highlighting contours in the resultant binary image (black and white). The gradient magnitude image must first be normalized to ensure all pixel values lie inside the range [0,1], which is the threshold's actual value. Although this approach, called global thresholding, is simple, it frequently fails.

Xi'an Shiyou Daxue Xuebao (Ziran Kexue Ban)/
Journal of Xi'an Shiyou University, Natural Sciences Edition
ISSN: 1673-064X
E-Publication: Online Open Access
Vol: 68 Issue 01 | 2025
DOI: 10.5281/zenodo.14752620

2.1 The Global Thresholding

In global thresholding with histograms, the image's histogram—which shows the distribution of pixel intensity values in the gradient image, is used to calculate the threshold value S. Keeping a certain proportion of the most noticeable contours is the aim of this method. For instance, the pixel percentage corresponding to the HIGHEST intensity values is determined using the gradient image's cumulative histogram if the objective is to preserve the top 20% of the strongest contours. Following this decision, the threshold value S will be used in the binarization procedure.

2.2 Local Thresholding by Hesterisis

Unlike the earlier thresholding techniques, this one, called local thresholding by hysteresis, employs different processing for each image pixel. Here, attention is drawn to the pixels surrounding the image's most important contours. While attempting to maintain their continuity, the goal is to preserve the image's strongest contours. Implementing the approach requires two thresholds: a low threshold of Sb and a high threshold of Sh. A high threshold is applied to choose the most important contours in the gradient module image. The final black-and-white image contains these features. Weaker contours in the image are highlighted by using the low threshold.

Algorithm

- Pixel extraction that is higher than Sh. These pixels are known as P1.
- Pixels between Sb and Sh are extracted. These pixels are known as P2.
- P1 and P2 pixel contours related to P1 pixels are chosen to be represented.

This procedure becomes challenging when selecting Sb and Sh thresholds. Occasionally, it could be practical to enforce a relationship between the two thresholds, such as Sb=k* Sh, where K is the scaling factor. Depending on the use case, k is manually chosen, ranging from 0 to 1.

2.3 Adaptative Thresholding

Global thresholding entails establishing a single decision threshold above which pixels are categorized as foreground (the object) and below which pixels are classified as background. Conversely, adaptive thresholding uses a threshold that dynamically changes in various image regions, making it especially useful for managing illumination changes.

While global thresholding uses the histogram to separate peaks that indicate the object and background, adaptive thresholding uses a unique threshold for each region to identify the foreground object from the background. In particular, local adaptive thresholding is perfect for images that lack clear peaks in their histogram because it finds a unique threshold for each central pixel depending on its immediate neighborhood.

Xi'an Shiyou Daxue Xuebao (Ziran Kexue Ban)/
Journal of Xi'an Shiyou University, Natural Sciences Edition
ISSN: 1673-064X
E-Publication: Online Open Access
Vol: 68 Issue 01 | 2025
DOI: 10.5281/zenodo.14752620

3. METHOD

Recent iris segmentation techniques [18] frequently employ the Hough Transform and local hysteresis thresholding to detect edge maps and delineate the iris and pupil boundaries. In our novel thresholding approach, we determine the two thresholds used in local hysteresis thresholding as follows: T2 = k * T1, where Otsu's approach is used to determine the higher threshold (T1), and k is a scaling factor specified in the algorithm.

3.1 Algorithm Otsu_Hysteresis_Thresholding (Image, K):

T1←graythresh(image) // Calculate Otsu thresholding

T2←k×T1 // Calculate T2 by multiplying T1 with k

Ensure k∈(0,1)

bw←column vector of the image

pix←indices where bw>T1

Initialize stack with indices from pix

Create array O of neighbor offsets

While the stack is not empty:

Pop v from the stack

For each neighbor of vv based on O:

If neighbor > T2, add to stack and mark as edge

Reshape the image and return the segmented output

The segmented iris is then normalized using the Daugman Rubber Sheet Model [19] for pupil contraction, dilation, and iris and pupil non-concentricity. The Gabor filter [20] extracts features from the normalized iris to obtain an iris code. Lastly, using Hamming distance, the iris codes of the left and right eyes are combined at the score level. In our earlier work, we employed a score-level fusion technique called Dezert Smarandache [21].

3.2 Iris Segmentation

We use three methods to define the iris and pupil boundaries during the segmentation phase:

- Whole Iris Disk: The entire structure of the iris disk is considered while segmenting it.
- The Iris disk's two sides: Each of the two segments that make up the iris disk spans a 45° angle from the central axis.
- Only 50% of the iris disk is segmented, with only half of the disk being examined.

Xi'an Shiyou Daxue Xuebao (Ziran Kexue Ban)/
Journal of Xi'an Shiyou University, Natural Sciences Edition
ISSN: 1673-064X
E-Publication: Online Open Access
Vol: 68 Issue 01 | 2025
DOI: 10.5281/zenodo.14752620

3.3 Score Level Fusion Technique

The fusion problem is deciding when there is a partial conflict between two individuals' left and right iris. (We can have the same left iris of two individuals and a different one for the right iris $\Theta = \{\theta_1, \theta_2\}$: represents the finite set of hypotheses that define the fusion problem. Where

$$D^{\Theta} = \{0, \theta_1, \theta_2, \theta_1 \cup \theta_2, \theta_1 \cap \theta_2\} \quad (2)$$

θ_1: The hypothesis assumes that the left iris of two individuals is identical.

θ_2: The hypothesis assumes that the right iris of two individuals is identical.

$\theta_1 \cup \theta_2$: The hypothesis assumes that the left and right irises of two individuals are identical.

$\theta_1 \cap \theta_2$: The hypothesis assumes that the left and right irises of two individuals are different

The classic DSm (DezertSmarandache model) combination rule [20] is described as follows:

$$m(C) = \sum_{\theta_1 \cap \theta_2 = C} m_1(\theta_1)\, m_2(\theta_2) \ , \forall\, C \in D^{\Theta} \quad (3)$$

The DSmc theory effectively combines two sources of evidence, even if they do not agree (presence of partial conflict).

The classic DSm (Dezert Smarandache model) algorithm is described in [22]

4. RESULT AND DISCUSSION

4.1 Casia-IRISV4 Interval Database

In the CASIA-IrisV4 Interval database [23], 249 individual iris images with a grayscale resolution of 320x280 pixels were taken in a controlled environment. Each subject's images were collected over two sessions to add temporal changes and examine the stability of iris recognition algorithms. This dataset is invaluable for examining the iris's fine texture and evaluating the reliability of biometric devices.

We conducted our experiments on 120 individuals, each having five left and five right iris images, from the CASIA-IrisV4 Interval database.

4.2 Evaluation Criteria

False accept rate (FAR), equal error rate (EER), Accuracy (recognition rate), and false reject rate (FRR) were among the evaluation criteria used to assess the suggested approaches.

FRR: The percentage of individuals the system should recognize but reject is indicated by this rate.

Xi'an Shiyou Daxue Xuebao (Ziran Kexue Ban)/
Journal of Xi'an Shiyou University, Natural Sciences Edition
ISSN: 1673-064X
E-Publication: Online Open Access
Vol: 68 Issue 01 | 2025
DOI: 10.5281/zenodo.14752620

FAR: This rate shows the percentage of individuals the system admits despite assuming their identity is unknown.

EER: Using the first two rates previously indicated, this rate—a standard performance metric—is calculated. At this moment, FRR = FAR, the ideal ratio of false rejections to false acceptances is reached.

4.3 Method Analysis

First, to identify the best approach, we assessed the performance of the three segmentation approaches: the whole iris disc, both sides of the iris disc, and half of the iris disc.

Table 1: Iris segmentation techniques

	The Score level fusion method		
	DST [24]	**DSmc**[22]	**PCR5** [25]
Accuracy (%)	94.94	98.55	93.26
FFR (%)	5.76	8.55	5.33
FAR (%)	5.05	1.39	6.74
EER (%)	7.01	9.37	7.19

Table I shows that the Accuracy of 98.55%, the False Acceptance Rate (FAR) of 1.39%, the False Rejection Rate (FRR) of 8.55%, and the Equal Error Rate (EER) of 9.37% are all achieved by treating the complete iris disk, which clearly performs better than the other methods. In light of these findings, the entire iris disk was chosen as the segmentation method.

Second, we used metrics like Accuracy, False Acceptance Rate (FAR), False Rejection Rate (FRR), and Equal Error Rate (EER) to evaluate the score-level fusion method's performance.

Table 2: The Score level fusion method

	Iris Segmentation techniques		
	Whole iris disc	**Both side of iris disc**	**Half of iris disc**
Accuracy (%)	98.55	91.20	91.71
FFR (%)	8.55	7.11	4.66
FAR (%)	1.39	8.81	8.31
EER (%)	9.37	7.51	4.44

Table 2 shows that the DSmC method performs better than other score-level fusion methods, especially in terms ofaccuracy (98.55%), False Acceptance Rate (FAR: 1.39%), and False Rejection Rate (FRR: 8.55%). We therefore decided to use the Dezert-Smarandache Theory (DSmT) as the score-level fusion technique.

In the end, we contrasted several thresholding techniques, such as the proposed Otsu-Hysteresis approach, the Hysteresis approach, the Otsu method, and the Adaptive method.

Xi'an Shiyou Daxue Xuebao (Ziran Kexue Ban)/
Journal of Xi'an Shiyou University, Natural Sciences Edition
ISSN: 1673-064X
E-Publication: Online Open Access
Vol: 68 Issue 01 | 2025
DOI: 10.5281/zenodo.14752620

Table 3: Thresholding Methods

	Thresholding Methods		
	Accuracy (%)	**Accuracy (%)**	**Accuracy (%)**
Otsu method [2]	93.57	6.36	14.25
Hysterisis Method [26]	98.58	1.36	9.75
Adaptative method [15]	98.59	1.32	13
Otsu Hysterisis	94.06	5.83	20.41

Table 3 shows that adaptive thresholding exhibits good accuracy and positive outcomes for Equal Error Rate (EER), False Acceptance Rate (FAR), and False Rejection Rate (FRR). This technique is valuable for iris images taken in different lighting conditions since it determines a threshold for every pixel in the iris edge map. Hysteresis thresholding, which used two thresholds to precisely determine the contour in the iris edge map, also demonstrated equivalent performance. Furthermore, the accuracy of 93.57%, FAR of 6.36%, FRR of 14.25%, and EER of 17.08% were all satisfactory results of the Otsu method. With a 94.06% enhanced accuracy rate, the recently suggested Otsu Hysteresis approach improves the performance of the Otsu method, especially in terms of accuracy.

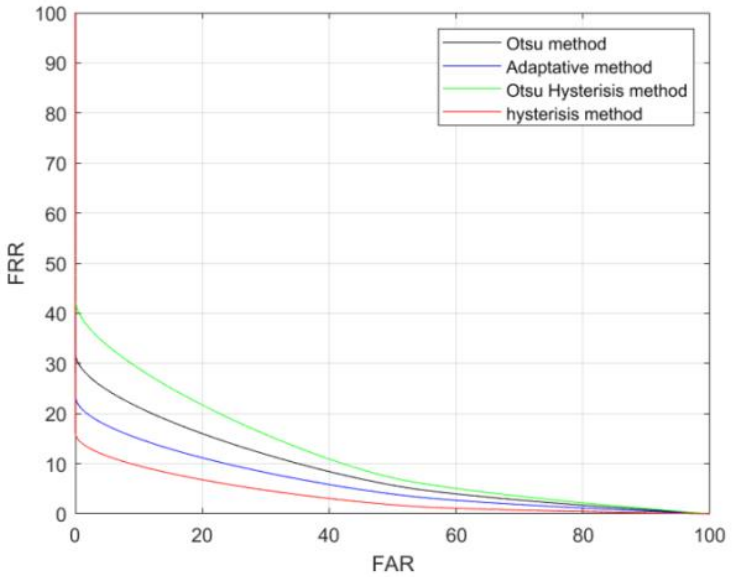

Figure 1: ROC Curve

As can be seen in figure 1, the adaptive and hysteretic approaches perform better since their ROC curves are closer to the origin than those of the other approaches. False Acceptance Rate (FAR) and False Rejection Rate (FRR) are decreased, accuracy is increased, and Equal Error Rate (EER) is decreased. A closer distance to the origin indicates a more accurate and balanced classification. In general, hysteretic and adaptive approaches are superior in reducing errors and improving performance.

Xi'an Shiyou Daxue Xuebao (Ziran Kexue Ban)/
Journal of Xi'an Shiyou University, Natural Sciences Edition
ISSN: 1673-064X
E-Publication: Online Open Access
Vol: 68 Issue 01 | 2025
DOI: 10.5281/zenodo.14752620

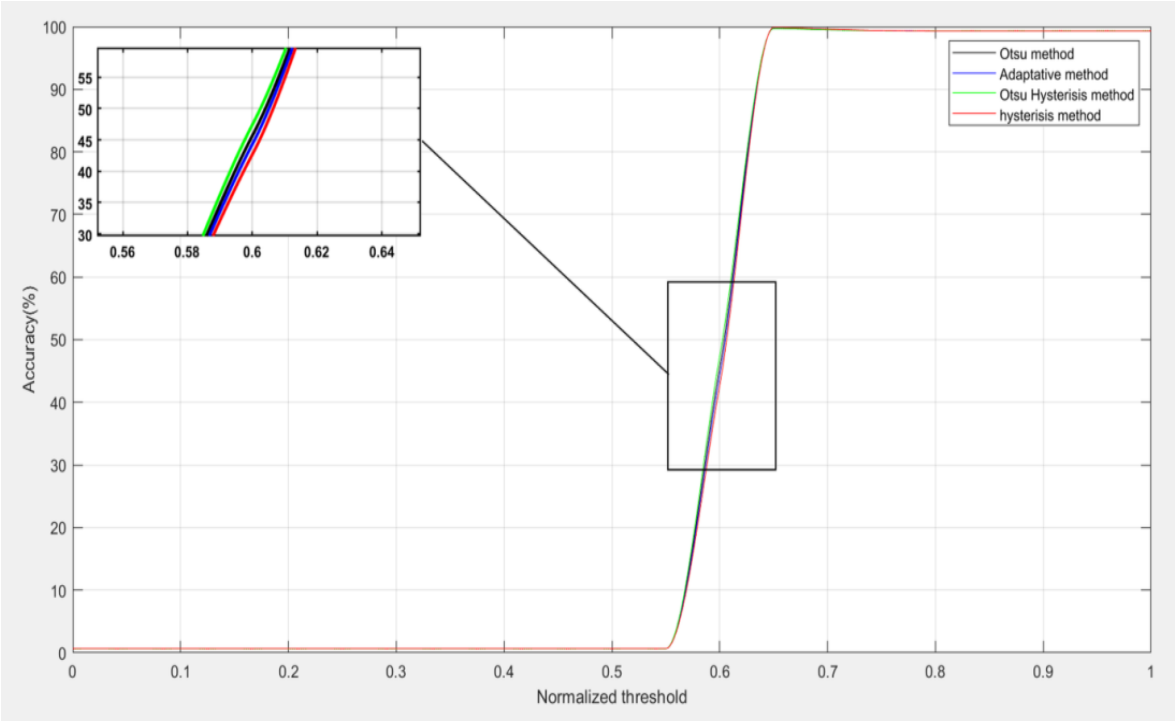

Figure 2: Accuracy Curve

The Hysteresis and Adaptive methods perform better than the others, as seen by their superior accuracy curves in figure 2. This is in line with the results in Table I, which regularly demonstrate superior outcomes for these approaches across a variety of evaluation parameters, validating their outstanding performance. The accuracy curves further show the resilience and dependability of these methods, showing how well they reduce classification errors. These findings offer compelling evidence of the effectiveness of the Hysteresis and Adaptive approaches in attaining increased accuracy.

5. CONCLUSIONS

In this paper, we present a new thresholding technique that combines Hysteresis local thresholding with the Otsu method. The whole iris disc is used to segment the iris. Dezert Smarandache's theory measures iris fusion at the score level. The CASIA-IrisV4 Interval database was used to assess the proposed method's efficacy. With an accuracy of 94.06%, a False Acceptance Rate (FAR) of 5.83%, a False Rejection Rate (FRR) of 20.41%, and an Equal Error Rate (EER) of 20.7%, the experimental result shows that the proposed method is competitive compared to previous thresholding techniques.

Acknowledgements

I dedicate this work to my late father: Pr. Mohamed Ghalem, a dedicated professor and researcher in history at the University of Oran, Algeria.

ISSN: 1673-064X
E-Publication: Online Open Access
Vol: 68 Issue 01 | 2025
DOI: 10.5281/zenodo.14752620

References

1) M. Yahiaoui, E. Monfrini, et B. Dorizzi, Markov Chains for unsupervised segmentation of degraded NIR iris images for person recognition, Pattern Recognition Letters, (2016);82:116-123, oct., doi: 10.1016/j.patrec.2016.05.025.

2) N. Otsu, A Threshold Selection Method from Gray-Level Histograms, IEEE Trans. Syst., Man, Cybern., (1979); 9(1): 62-66, doi: 10.1109/TSMC.1979.4310076.

3) Thresholding Using the ISODATA Clustering Algorithm, IEEE Trans. Syst., Man, Cybern., (1980);10(11):771-774, doi: 10.1109/TSMC.1980.4308400.

4) W. Q. Li et J. Z. Liu, The automatic thresholding of gray-level pictures via two-dimensional Otsu, Acta Automatica Sin, (1993):101-105.

5) A. Elen et E. Dönmez, Histogram-based global thresholding method for image binarization , Optik, (2024);306:171814, doi: 10.1016/j.ijleo.2024.171814.

6) A. Carolina Sparavigna, Tsallis Entropy In Bi-level And Multi-level Image Thresholding, ijSciences, (2015);1(1): 40-49,, doi: 10.18483/ijSci.613.

7) Jui-Cheng Yen, Fu-Juay Chang, et Shyang Chang, A new criterion for automatic multilevel thresholding, IEEE Trans. on Image Process., (1995);4(3):370-378, doi: 10.1109/83.366472.

8) C. H. Li et C. K. LEEt, Minimum cross entropy thresholding, Pattern Recognition, (1993);26(4): 617-625.

9) J. N. Kapur, P. K. Sahoo, et A. K. C. Wong, « A new method for gray-level picture thresholding using the entropy of the histogram », Computer Vision, Graphics, and Image Processing, (1985); 273-285.

10) R. Supriyanti, S. L. Dzihniza, M. Alqaaf, M. R. Kurniawan, Y. Ramadhani, et H. B. Widodo, Morphological features of lung white spots based on the Otsu and Phansalkar thresholding method, Indonesian Journal of Electrical Engineering and Computer Science, 2024;33(1) doi: 10.11591/ijeecs. v33.i1. pp530-539.

11) M.-T. Tran, Q.-N. Vo, et G.-S. Lee, Binarization of music score with complex background by deep convolutional neural networks, Multimed Tools Appl, (2021);80(7):11031-11047, mars, doi: 10.1007/s11042-020-10272-2.

12) M. Heikkila et M. Pietikainen, a texture-based method for modeling the background and detecting moving objects, IEEE Trans. Pattern Anal. Machine Intell., (2006); 28(4): 657-662, doi: 10.1109/TPAMI.2006.68.

13) J. Sauvola et M. Pietikäinen, Adaptive document image binarization, Pattern Recognition, (2000);33(2): 225-236, doi: 10.1016/S0031-3203(99)00055-2.

14) C. Eyupoglu, Implementation of bernsen's locally adaptive binarization method for gray scale images, (2017);7(2).

15) D. Bradley et G. Roth, Adaptive Thresholding using the Integral Image, Journal of Graphics Tools, (2007);12, nº 2, p. 13-21, janv., doi: 10.1080/2151237X.2007.10129236.

16) S. D. Yanowitz et A. M. Bruckstein, A new method for image segmentation, 9th International Conference on Pattern Recognition, Rome, Italy: IEEE Comput. Soc. Press, (1988); 270-275. doi: 10.1109/ICPR.1988.28220.

ISSN: 1673-064X
E-Publication: Online Open Access
Vol: 68 Issue 01 | 2025
DOI: 10.5281/zenodo.14752620

17) R. Supriyanti, M. Alqaaf, Y. Ramadhani, et H. B. Widodo, Morphological characteristics of X-ray thorax images of COVID-19 patients using the Bradley thresholding segmentation, Indonesian Journal of Electrical Engineering and Computer Science, (2021);24(2), doi: 10.11591/ijeecs. v24.i2. pp1074-1083.

18) A. Bendale, A. Nigam, S. Prakash, et P. Gupta, Iris Segmentation Using Improved Hough Transform, in Emerging Intelligent Computing Technology and Applications,304 D.-S. Huang, P. Gupta, X. Zhang, et P. Premaratne, Éd., in Communications in Computer and Information Science, vol. 304., Berlin, Heidelberg: Springer Berlin Heidelberg, (2012);408-415. doi: 10.1007/978-3-642-31837-5_59.

19) J. Daugman, How Iris Recognition Works, IEEE Transactions on Circuits and Systems for Video Technology, (2004);14(1): 21-30, janv., doi: 10.1109/TCSVT.2003.818350.

20) D. Gabor, Theory of communication. Part 1: The analysis of information, Journal of the Institution of Electrical Engineers - Part III: Radio and Communication Engineering, (1946);93(26): 429-441, doi: 10.1049/ji-3-2.1946.0074.

21) F. Smarandache, Advances and Applications of Dsmt for Information Fusion. Collected Works, (2023) ; 5.

22) K. G. Ghalem et A. Benouar, Alternative Techniques of Dempster-Shafer Theory for Iris Recognition », in 2024 2nd International Conference on Electrical Engineering and Automatic Control (ICEEAC), Setif, Algeria: IEEE, (2024);1-6. doi: 10.1109/ICEEAC61226.2024.10576411.

23) Iris Database, CASIA Iris Database V4. Consulté le : 2 décembre 2024. [En ligne]. Disponible sur : http://english.ia.cas.cn/db/201610/t20161026_169399.html

24) G. Shafer, A Mathematical Theory of Evidence turns 40, International Journal of Approximate Reasoning, (2016);79(7), doi: 10.1016/j.ijar.2016.07.009.

25) F. Smarandache et J. Dezert, Proportional Conflict Redistribution Rules for Information Fusion.

26) A. Bovik, The Essential Guide to Image Processing, J. Electron. Imaging, (2007);19(2), doi: 10.1117/1.3430078.